Int. J. Environ. Sci. Technol. (2015) 12:939–950
DOI 10.1007/s13762-013-0469-8

ORIGINAL PAPER

# Competitive adsorption of dye species from aqueous solution onto melon husk in single and ternary dye systems

**A. A. Olajire · A. A. Giwa · I. A. Bello**

Received: 28 April 2012 / Revised: 10 November 2013 / Accepted: 2 December 2013 / Published online: 9 January 2014


**Abstract** Polluted water may contain more than one dye species. Consequently, the behavior of a particular dye in a water system may be affected by the presence of the others. In this study, the adsorption of methylene blue (MB) in single dye system (SDS) and in ternary dye system (TDS) comprising of MB, congo red and methyl orange onto formaldehyde-treated melon husk (FMH) was investigated as a function of pH, contact time and species concentrations. Surface studies of FMH were investigated by Fourier transform infrared and scanning electron microscopy. The dye species adsorption equilibria were rapidly attained after 60 (SDS) and 90 min (TDS) of contact times. The adsorption kinetics were analyzed using pseudo first-order, pseudo second-order and intraparticle diffusion models and the adsorption data were well described by the pseudo second-order model. The equilibrium adsorption data were interpreted in terms of the Langmuir, Freundlich, Temkin, Dubinin–Radushkevich, Harkin–Jura and Halsey isotherm models and the goodness of fittings were inspected using linear regression analysis ($R^2$). Our results indicated that the Langmuir model was best fitted, suggesting monolayer adsorption. Thermodynamic study showed that the adsorptions in SDS and TDS on FMH are favourable. The change in entropy ($\Delta S°$) and heat of adsorption ($\Delta H°$) of dye species on FMH in TDS were estimated as 82.2 J/mol K and 17.95 kJ/mol. respectively while in SDS, they were respectively −43.76 J/mol K and −21.84 kJ/mol. The sorption process in both systems was thermodynamically feasible with negative $\Delta G°$ values.

**Keywords** Melon husk · Single dye system (SDS) · Ternary dye system (TDS) · Kinetics · Thermodynamics · Isotherms

A. A. Olajire (✉) · A. A. Giwa
Industrial and Environmental Chemistry Unit, Department of Pure and Applied Chemistry, Ladoke Akintola University of Technology, Ogbomosho, Nigeria
e-mail: olajireaa@yahoo.com

I. A. Bello
Physical Chemistry Unit, Department of Pure and Applied Chemistry, Ladoke Akintola University of Technology, Ogbomosho, Nigeria

## Introduction

Pollutants in water and wastewater have increased recently due to high increase in various industrial activities. Using dyes in many industries (Bulut et al. 2007) such as textile, paper, plastics, leather, food and cosmetic, represent a large group of chemicals that get mixed in wastewater among many aqueous pollutants. In recent years, there is a dramatic increase in the annual production of different synthetic dyes representing more than 10,000 dyes (ALzaydien 2009). Many azo dyes and their intermediates have toxic effects on environment and human health due to their carcinogenicity and visibility (Gong et al. 2005). It was reported that incomplete degradation of dyes by bacteria in the sediment of textile industry resulted in production of some carcinogenic and harmful amines (Vandevivere et al. 1998). Dyes usually have synthetic origin and complex aromatic molecular structures which make them to be stable and difficult to biodegrade (Zawani et al. 2009). They have inhibiting effect on the process of photosynthesis, thus affecting the aquatic ecosystem due to reduced light penetration, and may also be toxic to some aquatic life due to the presence of metals, chlorides, etc. in them; as well as inhibiting several biological processes (Karaca et al. 2008; Rangnathan et al. 2007).

Many treatment techniques have been applied to a broad range of water and wastewater contaminated with dyes including physical or chemical treatment processes (Crini 2008). These include chemical coagulation/flocculation (Mohammad and Muttucumaru 2009), ozonation, oxidation, photodegradation (Elmorsi et al. 2010). Many of these techniques are costly, required various tools and have limitations. It has been reported that the adsorption onto activated carbon, have proven to be the most efficient and reliable method for the removal of many pollutants, including different dyes (Aksu 2005; Senthilkumaar et al. 2005). Although commercial activated carbon is a very effective adsorbent, its high cost requires the search for alternatives and low-cost adsorbents (Pollard et al. 1992). Several low-cost adsorbents have been tested for removing dyes (Garg et al. 2004) including peat, pith, orange peel, Indian Rosewood (Pollard et al. 1992), cellulose based wastes, giant duckweed, banana pith and other agricultural by-products (Garg et al. 2004; Elmorsi 2011; Batzias and Sidiras 2007; Juang et al. 2007; Malik 2004; Namasivayam et al. 2001). On the other hand, seed husk of melon (*Citrillus lanatus*) is a common locally available agrowaste found widely in different areas in southwestern Nigeria, in addition to other parts of the country.

Melon husk is an agricultural waste material lying to be decayed and later constitute environmental nuisance, sometimes, of course used as domestic fuel as well. Little information is available in the literature on the use of melon husk as a natural adsorbent. The present study attempts to use seed husk of melon, as nonconventional low-cost adsorbent for adsorption of methylene blue (MB) in single dye system (SDS) and ternary dye system (TDS), comprising of a mixture of MB, congo red (CR) and methyl orange (MO) dyes from aqueous solution. The novelty in this work lies on the fact that several works have been done on the adsorption of SDS from aqueous solutions using agrowaste-based adsorbents, but not much work has been reported on the effect of the presence of other dye species on adsorption process, especially onto melon husk.

This work reports the results obtained on the ability of formaldehyde-treated melon husk (FMH) to remove MB from aqueous solution in SDS and in TDS. The influence of several operating parameters such as initial concentration, contact time, adsorbent dosage, pH and temperature was investigated. Equilibrium isotherms, kinetics and thermodynamic modelling were used to deduce the possible mechanism of the adsorption process.

## Materials and methods

### Adsorbent

Melon husk used in this work was obtained from local farm produce markets in Ogbomoso metropolis, Southwest Nigeria. Debris and other foreign materials were hand-picked from the husk, after which it was thoroughly washed with distilled water, drained and dried. The dried material was then ground and sieved before being treated with formaldehyde, following the methods of Azhar et al. (2005). The washed, dried and ground husk was soaked in 1 % formaldehyde in the weight ratio 1:5 at 50 °C for 4 h. This was to polymerize and immobilize the colour and soluble substances. Excess formaldehyde was drained and the husk was washed with distilled water to remove any free formaldehyde. It was then dried at 80 °C for 24 h. The adsorbent was sieved, and then stored in air tight container prior to analysis.

### Adsorbent characterization

The IR spectrum of the FMH was recorded with Nicolet Avatar 330 FT-IR in the range of 4,000–450 $cm^{-1}$ using KBr disk as reference (Fig. 1). The scanning electron

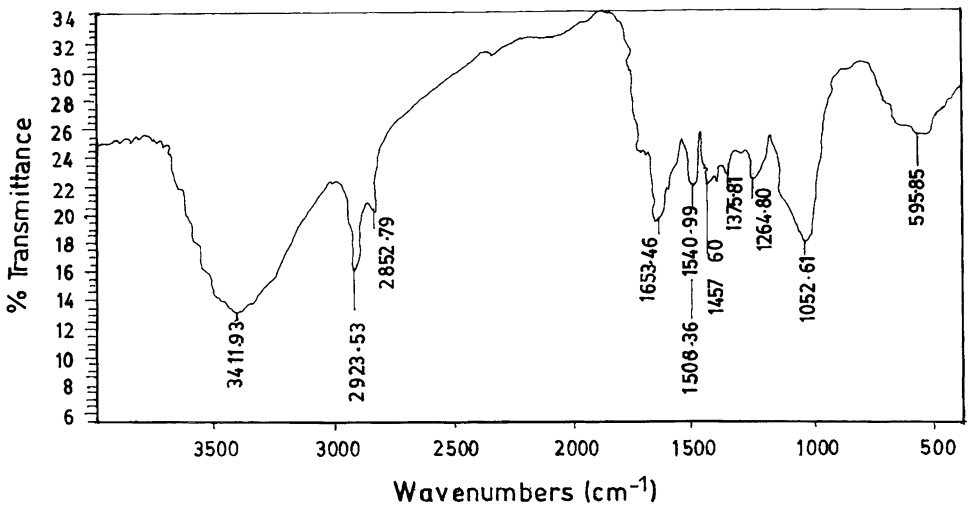


**Fig. 1** FTIR spectrum of FMH

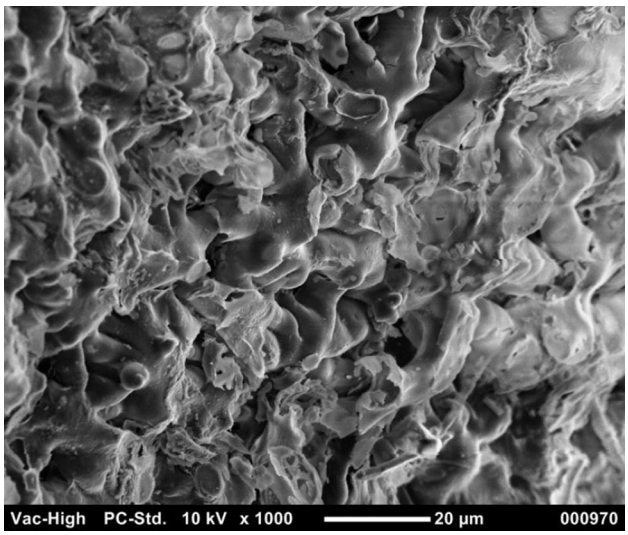


**Fig. 2** SEM images FMH at magnification ×1,000

**Table 1** Characteristics of the FMH

| Property | FMH |
|---|---|
| Density (g/cm$^3$) | 0.82 |
| Specific surface area (m$^2$/g) | 395 |
| Moisture content (%) | 3.97 |
| Ash content (%) | 5–7 |
| Solubility in water (%) | 0.50 |
| pH of 5 % slurry | 6.5 |

microscope (Hitachi 2300 Scanning electron microscope) was used to study the surface morphology of the adsorbent prepared from melon husk (Fig. 2). Samples were coated with gold before being subjected to SEM analysis.

All physico-chemical characteristics of the adsorbents were determined using standard methods (APHA, AWWA, WEF 1995; ISI 1989; Vogel 1969) and are presented in Table 1.

## Chemicals

All chemicals used in this study were of analytical-grade and used without further purification. The adsorbate used in this study was a mixture of three dyes : CR (by Timstar Laboratory Suppliers), MO (by BDH Chemicals) and MB (M & B Laboratory Chemicals); their chemical structures are given in Fig. 3. The dyes were obtained in commercial purity, and used without any further purification. Methylene blue dye alone (SDS) and in the presence of two acid dyes (TDS) was used as the model adsorbate in the present study to evaluate the efficiency of FMH as a natural adsorbent.

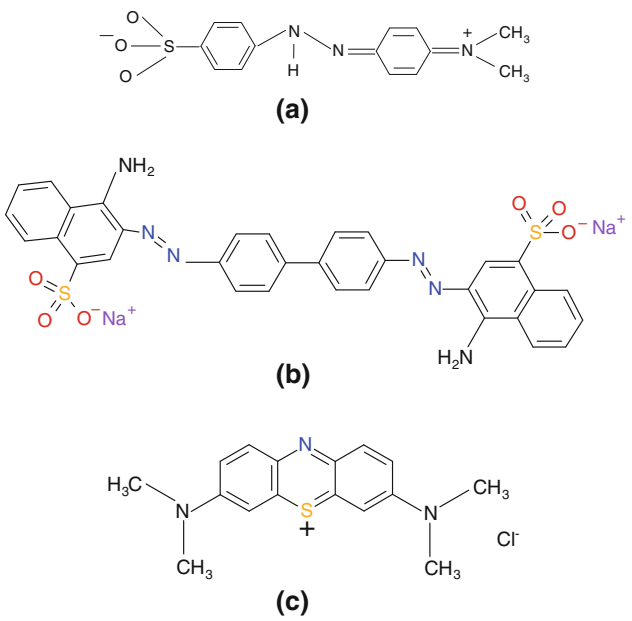


**Fig. 3** Chemical structures of MO (**3a**), CR (**3b**) and MB (**3c**)

## Adsorbate

Methylene blue alone and in the presence of CR and MO was used in this study as an environmental pollutant. A stock solution of each of them was prepared by dissolving 500 mg of the dye in distilled water to give a concentration of 500 mg/L solution. Experimental solutions of desired concentrations were prepared by mixing calculated volumes of the stock solutions of each dye and accurately diluting it with distilled water. Calibration curves were prepared by serial dilutions (1.0–10.0 mg/L).

## Adsorption studies

Batch adsorption experiments were conducted to study the guest–host interaction by shaking a series of glass bottles, each containing 25 mL solution of MB of desired concentrations. Then the bottles were tightly fixed in a horizontal thermostated shaker (SM 101 by Surgafriend Medicals) and were shaken with a known amount of adsorbent at 120 rpm for 80 min at room temperature. Shaking proceeded for 2 h to establish equilibrium, after which FMH in the samples was separated by centrifugation and the concentrations of MB at any time ($t$) were determined in the supernatant solutions using Genesys UV–Vis scanning spectrophotometer.

### *Effect of adsorbent dosage*

The effect of adsorbent dosage was studied by shaking different masses of FMH (0.025, 0.05, 0.10, 0.20, 0.30, 0.40, 0.50, 0.60, 0.65 and 0.70 g) with 25 mL of 50 mg/L

MB solution at 30 °C in a horizontal thermostated shaker (SM 101 by Surgafriend Medicals). Shaking proceeded for a time greater than their equilibrium time at 120 rpm at their natural pH, after which the dye solution was left to settle, and then filtered. The residual concentration of the dye solution was determined spectrophotometrically using Genesys 10 UV–VIS Scanning Spectrophotometer at $\lambda_{max}$ 664 nm of MB.

*Effects of initial methylene blue concentration and contact time*

Studies were carried out by shaking (SM 101 by Surgafriend Medicals) 0.10 g of FMH with 25 mL aqueous solution of MB of different concentrations (5–100 mg/L), at their natural pH and at room temperature (30 ± 2 °C) in 250 mL conical flask at 120 rpm.

*Effects of pH and temperature on methylene blue sorption*

The effects of the pH on the equilibrium uptake of the MB by FMH were investigated over a range of pH values at the initial dye concentration of 50 mg/L. Changes in the pH of the dye solution were adjusted with 0.1 M HCl or 1.0 M NaOH to attain a pH ranging from 3 to 10 for the dye. The suspensions were agitated for time intervals greater than the equilibrium time. For temperature studies, adsorption of 50 mg/L of dye by 100 mg of adsorbent was carried out at 30, 40 and 50 °C in thermostated horizontal shaker (SM 101 by Surgafriend Medicals).

*Adsorption of methylene blue in ternary dye system*

Adsorption behaviour from aqueous solution in TDS was studied by keeping the concentrations of each of the two acid dyes (CR and MO) at 5 mg/L and varying the concentration of MB in the range of 5–300 mg/L. The uptake capacity of MB by FMH in the presence of the two acid dyes was monitored as described for single dye system.

Analytical methods

The MB, CR and MO dyes were chosen as simple model systems of common dyes used in the industry. The species concentration in the samples was measured spectrophotometrically, using Genesys 10 UV–VIS Scanning Spectrophotometer at 664 nm. For each adsorption experiment, samples were withdrawn at predetermined time intervals, and the adsorbate (FMH) was separated by the centrifuge. Then concentrations of residual TDS solutions were measured by monitoring the absorbance changes at a wavelength of MB dyes ($\lambda = 664$ nm). The amount of MB sorbed (in both single and TDSs), $q_t$, at any time, $t$, was calculated from;

$$q_t = \frac{(C_o - C_t)V}{W}. \tag{1a}$$

At equilibrium, $q_t = q_e$ and $C_t = C_e$; therefore, the amount of sorbed (in both single and in TDSs), $q_e$, was calculated from:

$$q_e = \frac{(C_o - C_e)V}{W} \tag{1b}$$

where $C_o$, $C_t$ and $C_e$ are the initial concentration ($t = 0$), concentration at any time ($t = t$) and equilibrium concentrations of dye solution (mg/L), respectively; $V$ is the volume of the solution (L) and $W$ is the mass of adsorbent (g) (Aboul-Fetouh et al. 2010). The MB removal percentage was calculated as follows:

$$Sorption,\ R\,(\%) = \frac{C_o - C_t}{C_o} \times 100. \tag{2}$$

Equilibrium isotherm modelling

The experimental data at equilibrium between the amount of adsorbed dye (in single and TDSs) ($q_e$) on the adsorbent (FMH) and the concentration of dye solution ($C_e$) at a

**Table 2** Different isotherm models used in this study and their linear forms

| Isotherm | Nonlinear form | Linear form | Plot | |
|---|---|---|---|---|
| Langmuir-I | $q_e = \frac{K_L C_e}{1 + K_L C_e}$ | $\frac{C_e}{q_e} = \left(\frac{1}{K_L q_m}\right) + \left(\frac{C_e}{q_m}\right)$ | $\frac{C_e}{q_e}$ versus $C_e$ | (3) |
| Freundlich | $q_e = K_f C_e^{1/n}$ | $\log q_e = \log K_f + \frac{1}{n}\log C_e$ | $\log q_e$ versus $\log C_e$ | (4) |
| Temkin | $q_e = ((RT/b) In\,(A \cdot C_e))$ | $q_e = \beta\, In\, K_T + \beta\, In\, C_e$ | $q_e$ versus $In\, C_e$ | (5) |
| D–R | $q_e = q_s e^{(-K_D \varepsilon^2)}$ | $In\, q_e = In\, q_s - K_D\, \varepsilon^2$ | $In\, q_e$ versus $\varepsilon^2$ | (6) |
| H–J | – | $\frac{1}{q_e^2} = \left(\frac{B}{A}\right) - \left(\frac{1}{A}\right) \log C_e$ | $\frac{1}{q_e^2}$ versus $\log C_e$ | (7) |
| Halsey | – | $In\, q_e = (1/n\, InK) - (1/n\, In\, C_e)$ | $In\, q_e$ versus $In\, C_e$ | (8) |

Where $q_m$ is the maximum capacity of adsorption in mg/g; $K_L$ is a constant related to the affinity of the binding sites in L/mg; '$K_f$' and '$n$' are the measures of adsorption capacity and intensity of adsorption; $\beta = (RT)/b_T$, is the Temkin constant; $T$ is the absolute temperature in $K$; $R$ is the universal gas constant; $b_T$ is related to the heat of adsorption in kJ/mol.; $K_T$ is the equilibrium binding constant in L/mol.; $q_s$ is the D–R isotherm constant in mg/g; $\varepsilon$ represents the Polanyi potential constant in kJ mol$^{-1}$; $A$ and $B$ are Harkin–Jura isotherm parameter and constant

constant temperature and pH were used to describe the optimum isotherm model. The linear forms of Langmuir (1918), Freundlich (1906), Temkin and Pyzhev (1940), Dubinin and Radushkevich (1947), Harkins and Jura (1944) and Halsey (1948) isotherm models equations (Table 2; Eqs. 3–8) were used to describe the equilibrium data. Applicability of these equations was compared by judging with the correlation coefficients ($R^2$). In this work, adsorption isotherm experiments were carried out at initial dye concentrations of 5–300 mg/L.

### Error functions

The usual way to validate a model is to consider the goodness-of-fit using the linear regression coefficients, $R^2$. However, using only the linear regression method may not be appropriate for comparing the goodness of fit of kinetic models (Ho 2004; Ho et al. 2005a, b; Kinniburg 1986). This is because an occurrence of the inherent bias resulting from linearization may affect the deduction (Din and Hameed 2010). Therefore, in this study in addition to the linear regression analysis, the experimental data were tested with sum-of-square error (SSE) (Wang et al. 2009) to determine the best fitting kinetic model. The error function is given by:

$$SSE = \sqrt{\frac{\sum \left(q_{e,\exp} - q_{e,\mathrm{calc}}\right)^2}{N}} \quad (9)$$

where $q_{e,\ \exp}$ is the experimentally determined sorption capacity; $q_{e,\mathrm{calc}}$ is the theoretical sorption capacity from the different kinetic models and $N$ is the number of data points.

## Results and discussion

### Adsorbent characterization

The Fourier transform infrared (FTIR) spectrum of FMH (Fig. 1) displays a number of absorption peaks, indicating the complex nature of the material under study. The FTIR spectroscopic analysis indicated broad bands at 3,411 $cm^{-1}$ representing bonded –OH or –NH groups. The band observed at 2,923 $cm^{-1}$ could be assigned to stretching of C–H bond of methyl and methylene groups. The band observed at 1,653 $cm^{-1}$ was assigned to a carbonyl bond of carboxylic acid in conjugation with the aromatic moiety and/or with intermolecular hydrogen bond. The peak observed at 1,540 $cm^{-1}$ was assigned to C=C stretching vibration while the peak at 1,508 $cm^{-1}$ corresponds to secondary amine group. The bands observed at 1,475 and 1,375 $cm^{-1}$ could be assigned to symmetric bending of $CH_3$. The peak observed at 595 $cm^{-1}$ could be due to C–X stretching vibration of an acyl halide (Olajire 2012). Thus, the FTIR analysis indicates that the FMH is represented by functional groups such as N–H, COOH, CO, C–X, and C=C that could be potential adsorption sites for interaction with both the cationic and anionic mixed dyes of ternary system.

The scanning electron microscope (SEM) was used to study the surface morphology of the adsorbent (Fig. 2). The textural structure of FMH was presented as scanning electron micrographs (of magnification 1,000×). Studies on the adsorbent's surface topography could provide important information on the degree of interaction between the adsorbent particles and the dye molecules (Mas Rosemal and Kathiresan 2009). The SEM images of the adsorbent showed the irregular texture and porous nature of the surface of FMH (Fig. 2). The seemingly rough surface of the adsorbent is an indication of high surface area (Demirbas et al. 2004).

The physico-chemical characteristics of FMH are listed in Table 2. The density and specific surface area of FMH were measured to be 0.82 $g/cm^3$ and 395 $m^2/g$. Other parameters such as moisture content, ash content, solubility in water and solution pH were determined to be 3.97, 5–7, 0.50, and 6.5 % respectively. As seen in the SEM (Fig. 2), the high surface area and the rough surface are requisite for an effective adsorbent.

### Effect of adsorbent dosage and pH

The dependence of adsorption of the MB on the concentration of FMH was investigated by varying the quantity of the adsorbent from 0.025 to 0.70 g in 25 mL of 50 mg/L solution of the dye while keeping other parameters (contact time, agitation speed, particle size, temperature) constant. As shown in Fig. 4a, adsorption density decreased from 39.09 to 4.14 mg/g for an increase in adsorbent mass from 0.025 to 0.3 g, whereas the percentage color removal increased from 78.18 to 99.27 % with the same increase in adsorbent mass. This observation is usually attributed to the increase in the adsorbent pore surface areas and availability of more adsorption sites with increasing mass of adsorbent (Azhar et al. 2005; Esmaeili et al. 2008).

The adsorption of MB by FMH were studied at various pH values of the MB solution (dosage 0.10 g, concentration 50 mg/L), obtained by addition of varying proportions of 0.1 M HCl or 1.0 M NaOH. The effect of pH on MB adsorption arose apparently from the charge properties of both MB and FMH. It is recognized that oxygen-containing functional groups are present on the surface of FMH. These functional groups are subject to protonation/deprotonation, depending on pH (Zawani et al. 2009). An increase in pH usually results in surface functional groups partially (or fully) deprotonated and thus a loss of positive charge and/

or buildup of negative charge. Figure 4b reveals that an increase in pH from 3 to 10 increases MB adsorption by FMH. The adsorptive increment resulted clearly from the deprotonation of the functional groups on the surface of FMH. The deprotonation resulted in an increased blockage of FMH surface by water molecules associated with negative charge. When the pH of MB solution was increased from 3 to 10, its adsorption increased from 8.92 to 14.49 mg/g. The uptake of MB increased suddenly after pH of 7 and was almost constant in the pH range 8–10. This result could be explained considering the electrostatic interaction between the surfaces of the adsorbent, negatively charged sites, mainly due to $COO^-$ species, with the cationic dye MB. Thus, at pH values ranging from 7 to 10; the $COO^-$ groups are available to adsorb the positively charged dyes, and thus increase the removal of MB from aqueous solution. Also, at low pH values, the presence of $H^+$ ions in the system makes the surface of the adsorbent to be protonated, thus acquiring positive charge, which then repels the basic dye cation electrostatically (Santhi et al. 2010). It is thus inferred that MB was primarily adsorbed on the negative surface of FMH at high pH.

## Effects of initial MB concentration (in SDS and TDS) and contact time

A FMH dosage of 0.10 g was added to 0.025 L of different concentrations (5–100 mg/L dye solution). Experiments were conducted at a temperature of 30 °C for 90 min to test the effect of initial concentration and contact time on the adsorption process. The results (Fig. 5a, b) indicated that the adsorption of MB (in SDS and TDS) onto FMH increases as $[MB]_o$ increased. This may be due to an enhanced interaction between the dye molecules and the surface of the adsorbent (guest–host interaction) with increasing initial concentration of the MB (Haris and Sathasivam 2009). An increase in adsorption capacity from 12.34 to 23.96 mg/g for example, was observed when the

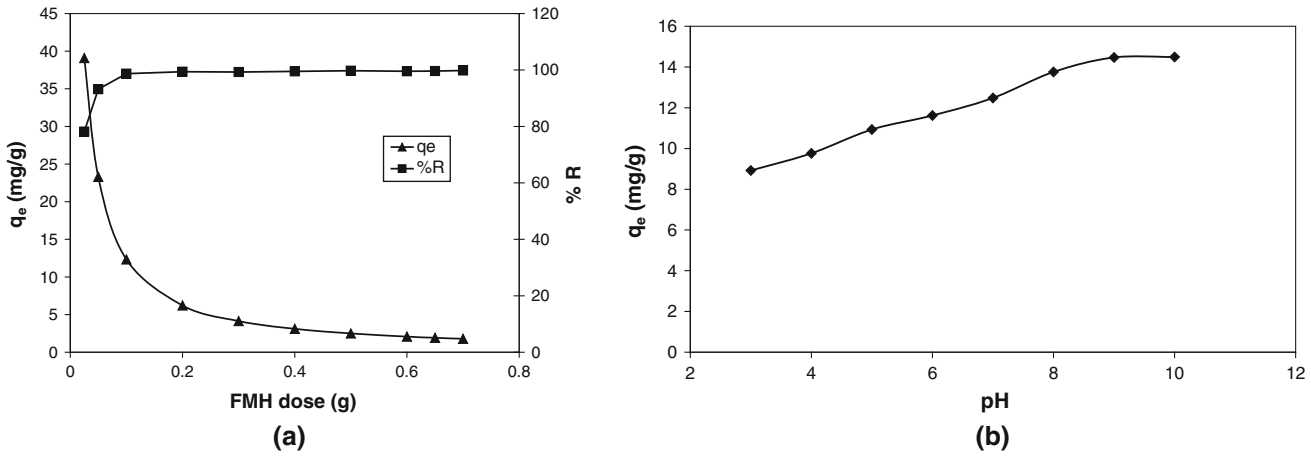


**Fig. 4** Effect of adsorbent dosage (**a**) and pH (**b**) on adsorption of MB in SDS

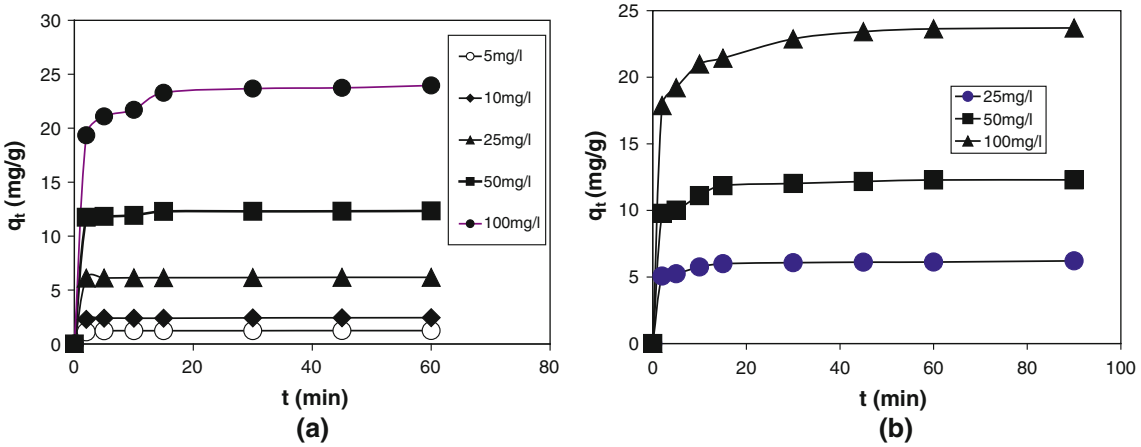


**Fig. 5** Effect of initial MB concentrations and contact time of MB in SDS (**a**) and TDS (**b**)

initial concentration of MB in SDS increased from 50 to 100 mg/L (Fig. 5a). A similar trend was also observed in TDS (Fig. 5b), but with slight decrease in the adsorption capacity (i.e. from 12.29 to 23.70 mg/g) which might be due to additional guest–guest interaction between MB and the two acid dyes that are present in the system.

Also, as the contact time increased to 30 min, $q_t$ in SDS increased by more than triple-folds (from 6.16 mg/g at $[MB]_o$ of 25 mg/L to 23.67 mg/g at $[MB]_o$ of 100 mg/L) (Fig. 5a). In TDS, same trend was observed (from 6.07 mg/g at $[MB]_o$ of 25 mg/L to 22.88 mg/g at $[MB]_o$ of 100 mg/L) (Fig. 5b). The adsorption of MB was very rapid during the first 10 min in both systems; and increased gradually during the second 30 min until equilibrium was reached at 60 and 90 min for SDS and TDS respectively. The results showed that the uptake of MB by FMH in the adsorption systems depends on $[MB]_o$ and contact time. This is because $[MB]_o$ act as the driving force that increases the mass transfer of the dye from aqueous solution onto the surface of FMH.

## Adsorption kinetics

In order to study the adsorption of MB in SDS and TDS onto FMH and to interpret the results, experimental data obtained were fitted to different kinetic models such as the pseudo-first-order (Annadurai et al. 2002), the pseudo-second order (Ho and Mckay 1999; Hameed et al. 2007) and an intraparticle diffusion (Annadurai et al. 2002; Weber and Morris 1963).

The rate constant of adsorption is determined from pseudo first-order equation given by Lagergren (1898), which is expressed as;

$$\log (q_e - q_t) = \log q_e - \left(\frac{k_1}{2.303}\right) t \tag{10}$$

where $q_e$ and $q_t$ are the amounts of MB adsorbed (mg/g) in both systems at equilibrium and at time $t$ (min), respectively, and $k_1$ is the rate constant adsorption ($min^{-1}$). Values of $k_1$ and $q_e$ calculable from slope and the intercept of the plot of log ($q_e$–$q_t$) versus $t$ (not shown) at different concentrations are given in Table 3. In SDS, the results show that the values of $R^2$ were low and the experimental $q_e$ values do not agree well with the calculated values ($q_e$, cal.) (Table 3). In TDS however, though the values of $R^2$ were moderately high, the experimental $q_e$ values do not agree with the calculated values ($q_e$, cal.) (Table 3). The model is not able to describe the experimental data properly because of the poor linear correlation and high SSE values (Table 3). All these observations show that the adsorption of MB onto FMH in both systems does not follow first-order kinetics.

The pseudo second-order equation based on equilibrium adsorption (Ho and Mckay 1999; Hameed et al. 2007) can be expressed as;

$$\frac{dq}{dt} = k_2 (q_e - q_t)^2 \tag{11a}$$

$$or \quad \frac{t}{q_t} = \frac{1}{(k_2 q_e^2)} + \left(\frac{1}{q_e}\right) t \tag{11b}$$

where $k_2$ (g/mg min) is the adsorption rate constant of pseudo second-order adsorption rate. The value of $q_e$ and $k_2$ can be obtained from the slope and intercept of the plot of $t/q_t$ versus $t$ respectively. The plots (not shown) were linear for all different initial concentrations of MB studied in both SDS and TDS. The correlation coefficients obtained for the pseudo-second-order kinetic model in both systems are very high; and are close or equal to unity (0.99–1) for all the initial MB dye concentrations studied. There is also a very good agreement between the experimentally obtained and calculated values of $q_e$ and the low values of its SSE (Table 3).

The mechanism of the rate-limiting step in this sorption process is further investigated by fitting the experimental data into intra-particle diffusion plot (not shown). It is proposed that the uptake of the adsorbate (MB) by the adsorbent (FMH) varies almost proportionately with the square root of the contact time ($t^{1/2}$). Weber and Morris (1963) proposed the most-widely applied intra-particle diffusion equation for sorption system as;

$$q_t = k_{id} t^{1/2} \tag{12}$$

where $q_t$ is the amount of MB adsorbed per unit mass of adsorbent (mg/g) at a time $t$ and $k_{id}$ is the intra-particle

**Table 3** Adsorption kinetics parameters for the adsorption of MB on FMH in SDS and TDS

| First-order kinetics model | | | | | | Second-order kinetics model | | | | |
|---|---|---|---|---|---|---|---|---|---|---|
| $[MB]_o$ | $q_e$ (exp.) | $q_e$ (cal.) | $K_1$ | $R^2$ | SSE | $q_e$ (cal.) | $K_2$ | $h$ | $R^2$ | SSE |
| 5 | 1.24 | 0.08 | −0.06 | 0.44 | 1.16 | 1.24 | 7.34 | 11.25 | 1.00 | 0.00 |
| 10 | 2.44 | 0.23 | −0.06 | 0.57 | 2.21 | 2.44 | 2.10 | 12.52 | 1.00 | 0.00 |
| 25 | 6.18 (6.21) | 0.30 (1.33) | −0.04 (−0.06) | 0.33 (0.71) | 5.88 (4.88) | 6.19 (6.24) | 2.33 (0.21) | 89.29 (8.01) | 1.00 (0.99) | 0.01 (0.03) |
| 50 | 12.34 (12.29) | 1.19 (4.66) | −0.08 (−0.11) | 0.54 (0.91) | 11.15 (7.63) | 12.38 (12.42) | 0.39 (0.09) | 59.88 (13.59) | 0.99 (0.99) | 0.04 (0.13) |
| 100 | 23.96 (23.70) | 6.42 (9.15) | −0.04 (−0.08) | 0.62 (0.95) | 17.55 (14.55) | 24.21 (24.04) | 0.06 (0.03) | 32.47 (18.58) | 0.99 (0.99) | 0.25 (0.34) |

Values in parenthesis are kinetic parameters for TDS ([MB] + [CR] = [MO] = 5 mg/L)

[MB] = mg/L; $q_e$ = mg/g; $k_1$ = $min^{-1}$; $k_2$ = g $mg^{-1}$ $min^{-1}$; SSE = %; FMH dosage = 0.10 g; $T$ = 303 K; pH = 6.5 and $V$ = 0.025 L

**Table 4** Weber–Morris parameters for the adsorption of MB on FMH in SDS and TDS

| $[MB]_o$ (mg/L) | $k_{1d}$ (mg $g^{-1}$ $min^{-1/2}$) | $R^2$ | $k_{2d}$ ($\times 10^{-3}$) (mg $g^{-1}$ $min^{-1/2}$) | $R^2$ | $X_i$ |
|---|---|---|---|---|---|
| 5 | 0.04 | 0.70 | 1.20 | 0.79 | 1.23 |
| 10 | 0.04 | 0.66 | 6.40 | 0.99 | 2.39 |
| 25 | 0.01 | 0.94 | 9.50 | 0.91 | 6.11 |
| | (0.40) | (0.97) | (3.33) | (0.95) | (5.89) |
| 50 | 0.20 | 0.83 | 16.50 | 0.79 | 12.21 |
| | (0.81) | (0.95) | (6.71) | (0.81) | (11.70) |
| 100 | 1.49 | 0.96 | 124.80 | 0.89 | 22.96 |
| | (1.51) | (0.97) | (19.64) | (0.80) | (21.96) |

Values in parenthesis are for TDS ([MB] + [CR] = [MO] = 5 mg/L); FMH dosage = 0.10 g; $T$ = 303 K; pH = 6.5 and $V$ = 0.025 L

diffusion rate constant (mg/g $min^{-1/2}$). If the intra-particle diffusion is the mechanism of the adsorption process, then the plot of $q_t$ versus $t^{1/2}$ will be linear and if the plot passes through the origin, then the rate limiting process is only due to the intra-particle diffusion (Jadhav and Vanjara 2004). Otherwise, some other mechanism along with intra-particle diffusion is also involved (ALzaydien 2009). In order to take care of boundary layer resistance that might be involved during the early stages of sorption, the equation was then modified (Poots et al. 1976) as;

$$q_t = k_{id}\, t^{1/2} + X_i \tag{13}$$

where $X_i$ depicts the boundary layer thickness. The rate parameter $k_{id}$ and $X_i$ of stage $i$ can be obtained from the slope and intercept of straight line of $q_t$ versus $t^{1/2}$. The results (Table 4) indicated that the plots of $q_t$ versus $t^{1/2}$ were more linear for TDS than SDS over the whole time range. This may attributed to higher total dye concentrations due to the presence of the two acid dyes in TDS. Furthermore, it was observed that the intra-particle diffusion in both systems occurred in two stages. The first straight portion was attributed to the macropore diffusion (phase I) and the second linear portion was attributed to micro-pore diffusion (phase II) (Jadhav and Vanjara 2004). The intra-particle diffusion constants for these two stages ($k_{1d}$ and $k_{2d}$) are given in Tables 4. Results indicated that the adsorption of MB on FMH involved more than one process, and that the intra-particle transport, though an important factor in the sorption process, may not be the rate-limiting step because the linear plots (not shown) do not pass through the origin. Also, the rate constants of the intra-particle diffusion on FMH increased with increasing $[MB]_o$ in both systems; however, they were lower for TDS than SDS due to additional guest–guest interaction in the former.

## Adsorption isotherm

Isotherm parameters, evaluated from the linear plots (not shown) of equations (3–8) are illustrated in Table 5. The value of $q_m$, $K_L$ are presented in Table 5. The $q_m$ value for the Langmuir I isotherm are 42.02 mg/g (SDS) and 26.32 mg/g (TDS). The adsorption coefficients, $K_L$, related to the apparent energy (surface energy) of sorption, on FMH were found to be 0.28 (SDS) and 0.33 L/g (TDS). The $R^2$ (correlation coefficient) value of 1.00 indicated that the Langmuir isotherm is good for explaining the sorption of MB on FMH in both systems. The $q_m$ which indicates the efficiency of an adsorbent for an adsorbate was found to be lower in TDS than SDS, as a result of the competition between MB and the two acid dyes in the former.

To investigate the possible multilayer adsorption and non-linear energy distribution of the adsorption sites, the Freundlich isotherm was studied. The intercept value ($K_f$) and the slope $n$ (Table 5) were obtained from the linear plots of Freundlich isotherm (not shown) at 30 °C. The values of $R^2$ for Freundlich plots were 0.94 (SDS) and 0.90 (TDS). The values of $1/n$ were 0.35 (SDS) and 0.33 (TDS). The $K_f$ (ultimate adsorption capacity) values as calculated from the Freundlich isotherm were 9.55 (SDS) and 7.34 L/g (TDS). The values of $1/n$, ranging from 0 to 1, is a measure of adsorption intensity or surface heterogeneity that becomes more heterogeneous as its value gets closer to zero (Ketcha et al. 2007). A value for $1/n$ below 1 indicates a normal Langmuir adsorption isotherm, while $1/n$ above 1 is indicative of cooperative adsorption (Fytianos et al. 2000; Abia and Asuquo 2006).

Temkin adsorption was chosen to fit the equilibrium adsorption data. The parameters, $K_T$ and $b_T$ of the Temkin

**Table 5** Parameters of the isotherm models for the adsorption processes

| Isotherm | | SDS | | TDS | |
|---|---|---|---|---|---|
| Model | Parameter | Value | $R^2$ | Value | $R^2$ |
| Langmuir | $q_m$ (mg/g) | 42.02 | 1.00 | 26.32 | 1.00 |
| | $K_L$ (L/g) | 0.28 | | 0.33 | |
| Freundlich | $k_f$ (L/g) | 9.55 | 0.94 | 7.34 | 0.90 |
| | $n$ | 2.83 | | 3.07 | |
| Temkin | $b_T$ (kJ/mol) | $1.59 \times 10^{-3}$ | | $1.03 \times 10^{-3}$ | |
| | $K_T$ (L/g) | 56.62 | 0.93 | 87.69 | 0.97 |
| D–R | $q_s$ (mg/g) | 18.13 | | 15.00 | |
| | $K_D$ ($mol^2/kJ^2$) | $2.0 \times 10^{-8}$ | 0.74 | $2.0 \times 10^{-8}$ | 0.79 |
| H–J | $A$ | –8.80 | | 6.51 | |
| | $B$ | –1.03 | 0.57 | 1.15 | 0.62 |
| Halsey | $K$ | 6.38 | | 6.11 | |
| | $N$ | 2.83 | 0.94 | 3.06 | 0.90 |

equation have been calculated for MB adsorption in both systems (Table 5). The Temkin adsorption potential ($K_T$) values were found to be 56.62 (SDS) and 87.69 L/g (TDS). The Temkin constant ($b_T$) values, related to heat of sorption, were found to be $1.59 \times 10^{-3}$ (SDS) and $1.03 \times 10^{-3}$ kJ/mol (TDS). However, as per Ho (1995), the typical range of bonding energy for ion-exchange mechanism is 8–16 kJ/mol. Since the range of bonding energy associated with the adsorbent under study were found to be substantially low, the interaction between MB and FMH in both systems (Table 5) seems not have involved ion–exchange mechanism, but rather physisorption mechanism.

The Dubinin–Radushkevich model is often used to estimate the characteristic porosity and the apparent free energy of adsorption. The isotherm parameters from the linear plots of the isotherm (not shown) are given in Table 5. Although the adsorbent showed relatively lower $R^2$ values (0.74 for SDS and 0.79 for TDS) compared to the preceding models (i.e., Langmuir, Freundlich and Temkin isotherms), yet it is significant enough for deriving information regarding the adsorption. The values of sorption affinity ($q_s$) of MB for FMH, as per for Dubinin–Radushkevich model (D–R model), are 18.13 (SDS) and 15.00 mg/g (TDS). The calculated mean energy of adsorption, E, from the D–R isotherm, gives information about the chemical or physical properties of the sorption (Caperkaya and Cavas 2008). The calculated mean energy value of adsorption of MB by FMH adsorbent is low (5.0 kJ/mol) and this implies that the type of adsorption appears to be physical processes because chemisorption processes have adsorption energies greater than 20 kJ/mol (Caperkaya and Cavas 2008).

The Harkin–Jura expression of the value of the correlation coefficient were 0.57 (SDS) and 0.62 (TDS), providing very poor correlation for the experimental data of MB on FMH in both systems. Halsey's expression of the values of the correlation coefficient were 0.94 (SDS) and 0.90 (TDS), providing moderately good fits for the experimental data of MB adsorption on FMH in both systems.

The adsorption capacity of FMH is compared with those of other adsorbents of agricultural waste origin using $q_m$, the maximum monolayer coverage from Langmuir model, which is a measure of the efficiency of an adsorbent. The comparison of the $q_m$ values is given in Table 6. Our adsorbent did perform fairly well than others that have been previously reported (Bulut and Aydin 2006; De Oliveria Brito et al. 2010; ALzaydien 2009; Ncibi et al. 2007; Bhattacharya and Sharma 2005; Ansori and Mosayebzadeh 2010; Caparkaya and Cavas 2008; and Giwa et al. 2013) while it performed below other adsorbents reported by others (Elmorsi 2011; Ofomaja 2007; Salleh et al. 2011; Kannan and Sundaram 2001 and Olajire et al. 2013).

**Table 6** Comparison of adsorption capacities of some adsorbents for MB in single and TDSs

| Adsorbent | $q_m$ (*or* $Q_o$) (mg $g^{-1}$) | References |
|---|---|---|
| Wheat shells | 16.56 | Bulut and Aydin (2006) |
| Brazil nut shells | 7.81 | De Oliveria Brito et al. (2010) |
| Miswak leaves | 200 | Elmorsi (2011) |
| Natural Jordanian Tripoli | 16.62 | ALzaydien (2009) |
| Posidonia oceanica fibre | 5.56 | Ncibi et al. (2007) |
| Palm kernel fibre | 671.78 | Ofomaja (2007) |
| Neem leaf powder | 19.61 | Bhattacharya and Sharma (2005) |
| Raw Walnut tree sawdust | 19.41 | Ansori and Mosayebzadeh (2010) |
| Polypyrrole treated walnut sawdust | 34.36 | Ansori and Mosayebzadeh (2010) |
| Cysteseira barbatula kutzing (a brown alga) | 21.93 | Caparkaya and Cavas (2008) |
| Agrowaste mixture | 93.46 | Salleh et al. (2011) |
| Bamboo dust carbon | 143.20 | Kannan and Sundaram (2001) |
| Raw melon husk | 47.39 | Olajire et al. (2013) |
| Raw melon husk (ternary system) | 22.42 | Giwa et al. (2013) |
| FMH (SDS) | 42.02 | This study |
| FMH (TDS) | 26.32 | This study |

## Thermodynamic study

Thermodynamic considerations of an adsorption process are necessary to conclude whether the process is spontaneous or not. In this study, a series of experiments were conducted at 30, 40 and 50 to study the effect of temperature on the equilibrium capacity of the FMH for the adsorbate. The change in standard free energy, enthalpy and entropy of adsorbent were calculated using the following equations:

$$\Delta G^\circ = -RT\, In\, K_c \tag{14a}$$

where $R$ is gas constant and $K_c$ is the equilibrium constant and $T$ is the temperature in K.

According to van't Hoff equation,

$$\log_{10} K_c = \frac{\Delta S^\circ}{2.303\, R} - \frac{\Delta H^\circ}{2.303\, RT}. \tag{14b}$$

The plots of $\Delta G^\circ$ versus temperature, $T$, were linear and the values of $\Delta H^\circ$ and $\Delta S^\circ$ were determined from the slope and intercept of the plots (not shown) respectively. The evaluated values of $\Delta G^\circ$, $\Delta H^\circ$ and $\Delta S^\circ$ are listed in Table 7. The negative value of $\Delta H^\circ$ (–21.84 kJ/mol) for SDS show the exothermic nature of adsorption while this was endothermic

**Table 7** Thermodynamic parameters for the adsorption of MB onto FMH in SDS and TDS

| Temperature (K) | Thermodynamic parameters | | |
|---|---|---|---|
| | $\Delta G°$ (kJ/mol) | $\Delta S°$ (J/mol K) | $\Delta H°$ (kJ/mol) |
| 303 | –8.56 (–7.02) | | |
| 313 | –8.17 (–7.66) | –43.76 (82.20) | –21.84 (17.95) |
| 323 | –7.69 (–8.67) | | |

Values in parenthesis are thermodynamic parameters for TDS ([MB] + [CR] = [MO] = 5 mg/L)

($\Delta H° = 17.95$ kJ/mol) for TDS. The positive value of $\Delta S°$ (82.2 J/mol K) suggest the increased randomness at the solid/solution interface during the adsorption of MB on FMH in TDS, while degree of randomness decreased in SDS ($\Delta S° = -43.76$ J/mol K). The negative values of $\Delta G°$ for both systems (Table 7) indicate the spontaneous nature of adsorption of MB on FMH in SDS and TDS at 30, 40, and 50 °C.

## Conclusion

FMH was able to adsorb MB in both SDS (MB only) and TDS (a mixture of MB, CR and MO dyes) from aqueous solutions. The adsorption processes followed pseudo second-order kinetics and the mechanism involved is more than one process. The kinetic data will be useful for the fabrication and designing dye wastewater treatment plant. Furthermore, among the six different isotherm models, equilibrium adsorption data was best fitted with the Langmuir-I isotherm model, with maximum momolayer coverage of SDS higher than that of TDS. The sorption processes in the two systems were spontaneous with negative values of $\Delta G°$ at all temperatures investigated. The value of $\Delta H°$ was negative in SDS, indicating that it was an exothermic process, whereas it was positive in TDS, showing that the adsorption was endothermic. The $\Delta S°$ value was positive in TDS, indicating an increased randomness at the solid/liquid interface during the adsorption process, while it was negative in SDS, indicating decreased randomness at solid/liquid interface.

**Acknowledgments** The authors are grateful to the Technonologists at the University Central Research Laboratory (UCRL) of Ladoke Akintola University of Technology, Ogbomoso, for their technical assistance. We are also grateful to the Faculty of Pure and Applied Sciences of the University for partially financing this research project.

## References

Abia A, Asuquo ED (2006) Lead (II) and nickel (II) adsorption kinetics from aqueous metal solutions using chemically modified and unmodified agricultural adsorbents. Afr J Biotechnol 5(16):1475–1482

Aboul-Fetouh MS, Elmorsi TM, El-Kady JM, El-Adawi HA (2010) Water hyacinth stems a potential natural adsorbent for the adsorption of acid green 20 dye. Environ Sci Indian J 5(4):257–266

Aksu Z (2005) Application of biosorption for the removal of organic pollutants: a review. Process Biochem 40(3–4):997–1026. doi:10.1016/j.procbio.2004.04.008

ALzaydien AS (2009) Adsorption of methylene blue from aqueous solution onto a low-cost natural Jordanian Tripoli. Am J Appl Sci 5(1):197–208

Annadurai G, Juang SR, Lee JD (2002) Use of cellulose-based wastes for adsorption of dyes from aqueous solutions. J Hazard Mater 92(3):263–274

Ansori R, Mosayebzadeh Z (2010) Removal of basic dye methylene blue from aqueous solutions using sawdust and sawdust coated with polypyrrole. J Iran Chem Soc 7(2):339–350

APHA, AWWA, WEF. (1995) Standard methods for the examination of water and wastewater, 19th edn. Ann Arbor Science Publishers, Washington

Azhar S, Liew AG, Suhardy D, Hafiz KF, Hatim MDI (2005) Dye removal from aqueous solution by using adsorption on treated sugarcane bagasse. Am J Appl Sci 2(2):1499–1503

Batzias FA, Sidiras DK (2007) Dye adsorption by prehydrolysed beech sawdust in batch and fixed system. Bioresour Technol 98:1208–1217

Bhattacharya KG, Sharma A (2005) Kinetics and thermodynamics of methylene blue adsorption on neem (*Azadirachta indica*) leaf powder. Dyes Pigm 65:51–59

Bulut Y, Aydin H (2006) A kinetics and thermodynamics studies of methylene blue adsorption on wheat shells. Desalination 194(2):807–811

Bulut Y, Gozubenli N, Aydın H (2007) Equilibrium and kinetics studies for adsorption of direct blue 71 from aqueous solution by wheat shells. J Hazard Mater 144(1–2):300–306. doi:10.1016/j.jhazmat.2006.10.027

Caparkaya D, Cavas L (2008) Biosorption of methylene blue by a brown alga *Cystoseira barbatula* Kützing. Acta Chim Slov 55:547–553

Crini G (2008) Kinetic and equilibrium studies on the moval of cationic dyes from aqueous solution by sorption onto a cyclodextrin polymer. Dyes Pigm 77(2):415–426. doi:10.1016/j.dyepig.2007.07.001

De Oliveria Brito SM, Andrade HMC, Soares LF, De Azevedo RP (2010) Brazil nut shells as a new biosorbent to remove methylene blue and indigo carmine from aqueous solutions. J Hazard Mater 174(1–3):84–92

Demirbas E, Kobya M, Senturk E, Ozkan T (2004) Adsorption kinetics of chromium (VI) from aqueous solutions on the activated carbons prepared fro agricultural wastes. Water SA 30(4):533–539

Din ATM, Hameed BH (2010) Adsorption of mrthyl violet dye on acid modified activated carbon: isotherm and thermodynamics. J Appl Sci Environ Sanitation x(n):151–160

Dubinin MM, Radushkevich LV (1947) The equation of the characteristic curve of activated charcoal. Dokl Akad Nauk SSSR 55:327–329

Elmorsi TM (2011) Equilibrium isotherms and kinetic studies of removal of methylene blue dye by adsorption onto miswak leaves as a natural adsorbent. J Environ Prot 2:817–827

Elmorsi TM, Riyad YM, Mohamed ZH, Abd El Bary HM (2010) Decolorization of Mordant red 73 azo dye in water using $H_2O_2$/UV and photo-Fenton treatment. J Hazard Mater 174(1–3):352–358. doi:10.1016/j.jhazmat.2009.09.057

Esmaeili A, Ghasemi S, Rustaiyan A (2008) Evaluation of the activated carbon prepared of algae gracilaria for the biosorption of Cu(II) from aqueous solutions. Am-Euras J Agric Environ Sci 3(6):810–813

Freundlich HZ (1906) Over the adsorption in solution. J Phys Chem 57A:385–470

Fytianos K, Voudrias E, Kokkalis E (2000) Sorption desorption behaviour of 2,4-dichlorophenol by marine sediments. Chemosphere 40:3–6

Garg VK, Amita M, Kumar R, Gupta R (2004) Basic dye (methylene blue) removal from simulated waste-water by adsorption using Indian rosewood sawdust: a timber industry waste. Dyes Pigm 63(3):243–250. doi:10.1016/j.dyepig.2004.03.005

Giwa AA, Olajire AA, Bello IA (2013) Removal of basic dye from aqueous solution by adsorption on melon husk in single, binary and ternary system. Chem Process Eng Res 13:51–68

Gong R, Li M, Yang C, Sun Y, Chen J (2005) Removal of cationic dyes from aqueous solution by adsorption on peanut hull. J Hazard Mater 121(1–3):247–250. doi:10.1016/j.jhazmat.2005.01.029

Halsey G (1948) Physical adsorption on non-uniform surfaces. J Chem Phys 16:931–937

Hameed BH, Din ATM, Ahmad AL (2007) Adsorption of methylene blue onto bamboo-based activated carbon: kinetics and equilibrium studies. J Hazard Mater 141(3):819–825. doi:10.1016/j.jhazmat.2006.07.049

Haris MRH, Sathasivam K (2009) The removal of methyl red from aqueous solutions using banana pseudostem fibers. Am J Appl Sci 6(9):1690–1700

Harkins WD, Jura EJ (1944) The decrease of free surface energy as a basis for the development of equations for adsorption isotherms; and the existence of two condensed phases in films on solids. J Chem Phys 12:112–113

Ho YS (1995) Adsorption of heavy metals from waste streams by peat. Ph.D Thesis, The University of Birmingham, Birmingham, UK

Ho YS (2004) Selection of optimum isotherm. Carbon 42(10):2115–2116

Ho YS, McKay G (1999) Pseudo-second order model for sorption processes. Process Biochem 34(5):735–742. doi:10.1016/S0032-9592(98)00112-5

Ho YS, Chiu WT, Wang CC (2005a) Regression analysis for the sorption isotherms of basic dyes on sugarcane dust. Bioresour Technol 96(11):1285–1291. doi:10.1016/j.biortech.2004.10.021

Ho YS, Chiang TH, Hsueh YM (2005b) Removal of basic dye from aqueous solution using tree fern as a biosorbent. Process Biochem 40:119–124

ISI (1989) Activated carbon, powdered and granular—method of sampling and tests, IS 877. Bureau of Indian Standards, New Delhi

Jadhav DN, Vanjara AK (2004) Adsorption kinetics study: removal of dyestuff effluent using sawdust, polymerized sawdust and sawdust carbon-II. Indian J Chem Technol 11(1):42–50

Juang LC, Wang CC, Lee CK, Hsu TC (2007) Dyes adsorption onto organoclay and MCM-41. J Environ Eng Manag 17(1):29–38

Kannan N, Sundaram MM (2001) Kinetics and mechanism of removal of methylene blue by adsorption on various carbons—a comparative study. Dyes Pigm 51:25–40

Karaca S, Gurses A, Acikildiz M, Ejder M (2008) Adsorption of cationic dye from aqueous solutions by activated carbon. Microporous Mater 115:376–382

Ketcha MJ, Ngomo MH, Kouotou D, Tchoua NP (2007) Kinetic and equilibrium studies of the adsorption of nitrate ions in aqueous solutions by activated carbons and zeolite. Res J Chem Environ 11(3):47–49

Kinniburg DG (1986) General purpose adsorption isotherms. Environ Sci Technol 20(9):895–904

Lagergren S (1898) Zur theorie der sogenannten adsorption gelöster stoffe. Kungliga. Svenska vetenskapsakademiens 24(2):1–39

Langmuir I (1918) The adsorption of gases on plane surfaces of glass, mica, and platinum. J Am Chem Soc 40:1361–1403

Malik PK (2004) Dye removal from wastewater using activated carbon developed from sawdust: adsorption equilibrium and kinetics. J Hazard Mater 113:81–88. doi:10.1016/j.jhazmat.2004.05.022

Mas Rosemal HMH, Kathiresan S (2009) The removal of methyl red from aqueous solution using banana psuedostem fibers. Am J Appl Sci 6(9):1690–1700

Mohammad ME, Muttucumaru S (2009) Review of pollutants removed by electrocoagulation and electrocoagulation/flotation processes. J Environ Manag 90(5):1663–1679. doi:10.1016/j.jenvman.2008.12.011

Namasivayam C, Radhika R, Suba S (2001) Uptake of dyes by a promising locally available agricultural solid waste: coir pith. Waste Manag 21:381–387

Ncibi MC, Mahjoub B, Seffen M (2007) Adsorptive removal of textile reactive dye using Posidonia oceanica (L.) fibrous biomass. Int J Environ Sci Tech 4(4):433–440

Ofomaja AE (2007) Kinetics and mechanism of methylene blue sorption onto palm kernel fibre. Process Biochem 42:16–24

Olajire AA (2012) Principles and applications of spectroscopic techniques. Sina2tees Publications, 268 pp

Olajire AA, Giwa AA, Bello IA (2013) Adsorptive removal of methylene blue dye by melon husk: kinetic and isothermal studies. Pak J Sci Ind Res Ser A Phys Sci 56(3):151–164

Pollard SJT, Fowler GD, Sollars CJ, Perry R (1992) Low-cost adsorbents for waste and waste-water treatment: a review. Sci Total Environ 116(1–2):31–52

Poots VJP, Mckay G, Healy JJ (1976) The removal of acid dye from effluent using natural adsorbents—II wood. Water Res 10:1067–1070

Rangnathan K, Karunagaran K, Sharma DC (2007) Recycling of wastewater of textile dyeing industries using advanced treatment technology and cost analysis. Resour Conserv Recycl 50:306–318

Salleh MAM, Mahmoud DK, Al-Maamary EA (2011) Adsorption of basic dye from aqueous solution using mixture of agricultural waste (Maw): isotherm, kinetic studies and process design. J Adv Sci Eng Res 1:76–97

Santhi T, Manonmani S, Smitha T (2010) Kinetics and isotherms studies on cationic dyes adsorption onto Annona squmosa seed activated carbon. Int J Eng Sci Technol 2(3):287–295

Senthilkumaar S, Varadarajan PR, Porkodi K, Subbhuraam CV (2005) Adsorption of methylene blue onto jute fiber carbon: kinetics and equilibrium studies. J Colloid Interface Sci 284(1):78–82. doi:10.1016/j.jcis.2004.09.027

Temkin MI, Pyzhev V (1940) Kinetics of ammonia synthesis on promoted iron catalysts. Acta Physiochim URSS 12:327–356

Vandevivere PC, Bianchi R, Verstraete W (1998) Treatment and reuse of wastewater from the textile wet-processing industry: review of emerging technologies. J Chem Technol Biotechnol 144(1–2):300–306

Vogel AI (1969) A text book of quantitative inorganic analysis, 3rd edn. ELBS, London

Wang XS, Li Z, Tao SR (2009) Removal of chromium (VI) from aqueous solution using walnut hull. J Environ Manag 90: 721–729

Weber WJ, Morris JC (1963) Kinetics of adsorption on carbon from solution. J Sanil Eng Div Am Soc Eng 89:31–60

Zawani Z, Luqman CA, Thomas SYC (2009) Equilibrium, kinetic and thermodynamics studies: adsorption of remazol black 5 on the palm kernel shell activated carbon. Eur J Sci Res 37(1):67–76